ELSEVIER

Chemical Geology 192 (2002) 23–45

CHEMICAL GEOLOGY
INCLUDING
ISOTOPE GEOSCIENCE

www.elsevier.com/locate/chemgeo

Timing of accretion and collisional deformation in the Central Asian Orogenic Belt: implications of granite geochronology in the Bayankhongor Ophiolite Zone

Craig Buchan[a,*], Jörg Pfänder[b,1], Alfred Kröner[c,2], Timothy S. Brewer[a,3], Onongin Tomurtogoo[d,4], Dondov Tomurhuu[d,4], Dickson Cunningham[a,3], Brian F. Windley[a,3]

[a] *Orogenic Processes Group, Geology Department, University of Leicester, Leicester LE1 7RH, UK*
[b] *Max-Planck-Institut für Chemie, Abteilung Geochemie, Postfach 3060, D-55020 Mainz, Germany*
[c] *Institut für Geowissenschaften, Universität Mainz, 55099 Mainz, Germany*
[d] *Institute of Geology and Mineral Resources, P.O. Box 118, Enkh Taivan Avenue 63, Ulaanbaatar 210351, Mongolia*

Received 13 December 2001; accepted 24 June 2002

Abstract

Growing evidence suggests that the mechanism of Palaeozoic continental growth in Central Asia was by subduction–accretion with punctuated collisions that produced ophiolitic sutures between accreted blocks. The Bayankhongor ophiolite is the largest ophiolite in Mongolia and possibly all of Central Asia, and is interpreted to mark the collisional suture between the Baidrag and Hangai continental blocks. New $^{207}Pb/^{206}Pb$ zircon evaporation ages for granite plutons and dykes that intrude the ophiolite and its neighbouring lithotectonic units suggest that the ophiolite was obducted at c. 540 Ma at the beginning of a collisional event that lasted until c. 450 Ma. The new data, combined with that of previous studies, indicate regional correlation of isotopic ages north-westward from Bayankhongor to southern Tuva. These data record oceanic crust formation at c. 570 Ma, followed by approximately 30 million years of subduction–accretion that culminated in obduction of ophiolites, collision related metamorphism, and magmatism in the period c. 540–450 Ma. Correlation of isotopic-age data for the ophiolites of western Mongolia and southern Tuva suggests that the ophiolites define a major collisional suture in the Central Asian Orogenic Belt (CAOB) that defines the southern and western margins of the Hangai continental block.

Keywords: Central Asian Orogenic Belt; Zircon geochronology; Mongolia; Ophiolites

* Corresponding author. Present address: Tectonic Special Research Centre, Department of Applied Geology, Curtin University of Technology, GPO Box 1987, Perth 6845, Western Australia, Australia. Fax: +44-116-252-3918.

E-mail addresses: buchanc@lithos.curtin.edu.au (C. Buchan), pfaender@uni-muenster.de (J. Pfänder), kroener@mail.uni-mainz.de (A. Kröner), tsb5@le.ac.uk (T.S. Brewer), inst_geology@arvis.ac.mn (O. Tomurtogoo), inst_geology@arvis.ac.mn (D. Tomurhuu), wdc2@le.ac.uk (D. Cunningham), bfw@le.ac.uk (B.F. Windley).

[1] Fax: +49-6131-371-051.
[2] Fax: +49-6131-392-4769.
[3] Fax: +44-116-252-3918.
[4] Fax: +49-976-1-457858.

0009-2541/02/$ - see front matter © 2002 Elsevier Science B.V. All rights reserved.
PII: S0009-2541(02)00138-9

1. Introduction

The Central Asian Orogenic Belt (CAOB) is a complex collage of island arcs, continental blocks and fragments of oceanic crust that amalgamated during the Palaeozoic to Mesozoic. Recent studies provide growing evidence that continental growth occurred through a process of subduction–accretion with punctuated collisional events resulting in the formation of ophiolitic sutures between accreted blocks (Hsü et al., 1991; Mossakovsky et al., 1994; Buchan et al., 2001). However, despite an improved understanding of the crustal growth mechanisms, a paucity of reliable geochronological data has hindered correlation of sutures and collisional deformation within the orogen, or has led to questionable models based solely on lithological similarity. One such example is the grouping of high-grade gneiss terranes in western Mongolia and Tuva into a singular Archaean to Palaeoproterozoic continental block named the Tuva–Mongolian Massif (Mossakovsky et al., 1994; Dergunov et al., 1997). However, Kozakov et al. (1999) showed that granulite-facies gneisses in Tuva, previously assumed to represent part of the Tuva–Mongolian Massif, are early Cambrian in age (536±6 Ma, U–Pb single zircon). Miscorrelation has led to confusing regional relationships, and misunderstanding of the mechanisms of continental growth (see Lamb and Badarch, 1997; Buchan et al., 2001 for detailed discussion).

Mongolia occupies a central position within the Central Asian collage and is therefore pivotally located for understanding crustal growth in the region. This paper presents new zircon geochronological data from granites and rhyolite dykes that intrude the Bayankhongor ophiolite zone, which is the largest ophiolitic suture in Mongolia, and possibly all of Central Asia (Fig. 1, Buchan et al., 2001). The new data, combined with previously published K–Ar and Ar–Ar data from metamorphic micas associated with faults within the ophiolite zone (Teraoka et al., 1996; Kurimoto et al., 1998; Takahashi et al., 1998b; Delor et al., 2000; Höck et al., 2000), provide important constraints on the timing of obduction of the Bayankhongor ophiolite and subsequent deformation. In addition, it is demonstrated that the deformation events associated with creation of the Bayankhongor granites can be traced on a regional scale north-westward along-strike to Tuva, southern Siberia. The correlation of these deformation events suggests that they represent a major magmatic episode in the history of the CAOB.

2. Geological setting

The mechanism of continental crustal growth in Central Asia is the subject of current debate. Şengör et al. (1993) propose a mechanism of continuous continental growth through subduction accretion and arc collision. This model implies that a subduction zone existed along the southern margin of the Siberian craton throughout the Palaeozoic producing a vast complex of arc and subduction–accretion material including offscraped ophiolitic fragments in front of seaward-migrating magmatic fronts. In contrast, Coleman (1989), Hsü et al. (1991) and Mossakovsky et al. (1994) identify distinct ophiolite belts, which are interpreted as discrete suture zones between tectonic blocks. These models differ in that the former invokes steady state subduction–accretion over a prolonged period of time, whereas the latter favours punctuated accretion by collision and closure of multiple ocean basins now marked by ophiolitic sutures. In order to understand how the CAOB was formed, it is essential to work out the tectonic

Fig. 1. Map of ophiolite occurrences in Mongolia, the Bayankhongor ophiolite is the largest. Isotopic age data for the highlighted ophiolites demonstrates marked correlation of ophiolites created at around 570 Ma. The trace of basement structural grain indicates that these ophiolites occur along a gently curving semicontinuous belt. inset: Aeromagnetic map of central and western Mongolia (Mongolian Academy of Sciences, unpublished data). Areas of highest magnetism shown in white and lowest magnetism in dark grey. Black or striped areas have no data. The magnetic data define the margins of the unexposed Hangai continental block denoted by the symbol KHA, as an area with relatively low magnetism surrounded by more magnetic bodies, which correspond largely to ophiolite belts. The positions of the Bayankhogor, Khantai-shir, Dariv, Ozernaya (OZR), Aghardagh Tes-Chem and Dzhida (DZH) ophiolite belts are marked. Sources of age data: Bayankhongor (Kepezhinskas et al., 1991), Khantaishir and Dariv (Salnikova, personal communication), Ozernaya (Kovalenko et al., 1996a) and Agardagh Tes-Chem (Pfänder et al., 1999).

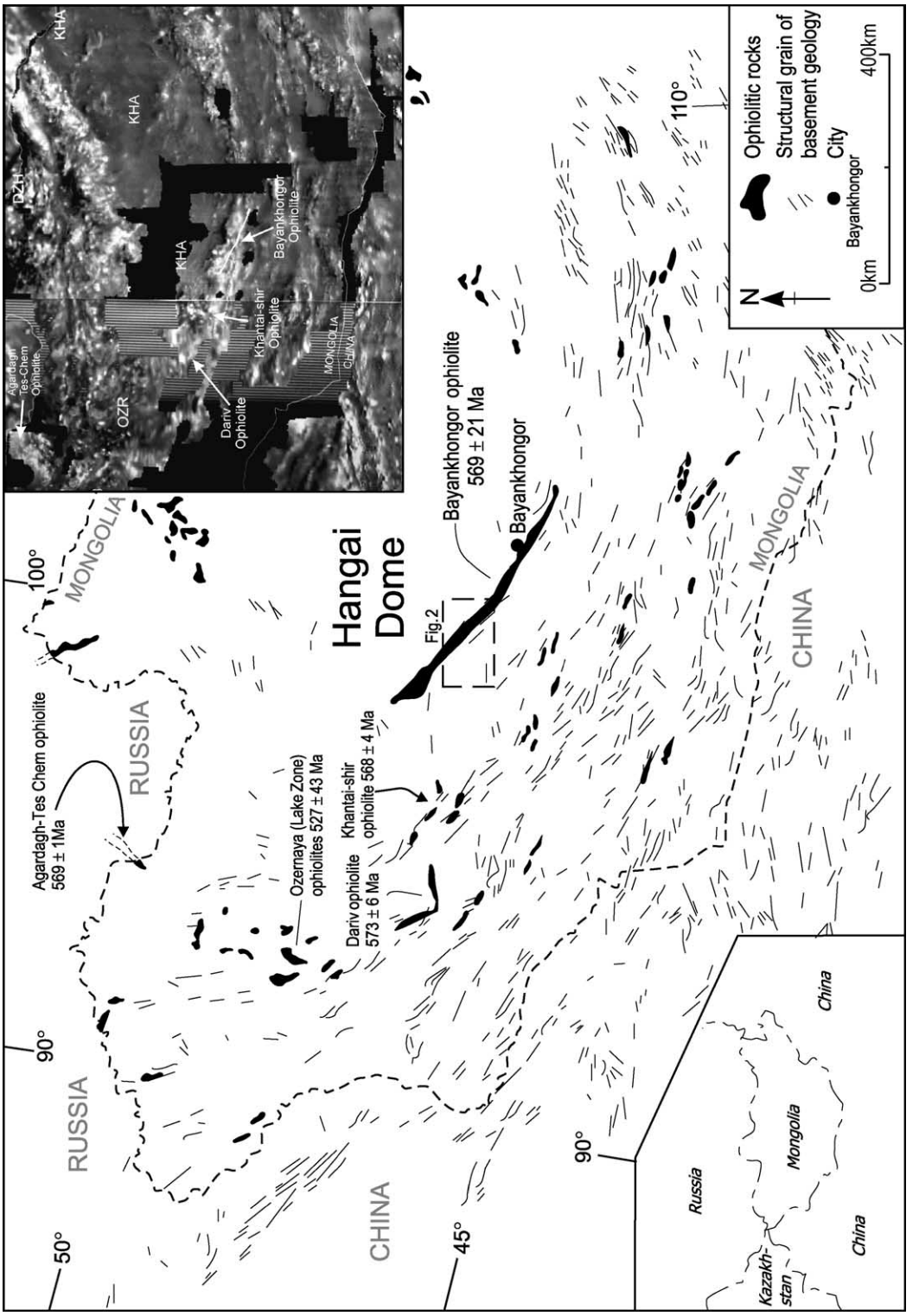
Agardagh-Tes-Chem Ophiolite
OZR
Dariv Ophiolite
Khantai-shir Ophiolite
Bayankhongor Ophiolite
KHA
DZH
MONGOLIA
CHINA
Hangai Dome
Agardagh-Tes Chem ophiolite 569 ± 1Ma
Ozernaya (Lake Zone) ophiolites 527 ± 43 Ma
Dariv ophiolite 573 ± 6 Ma
Khantai-shir ophiolite 568 ± 4 Ma
Bayankhongor ophiolite 569 ± 21 Ma
Bayankhongor
Fig. 2
RUSSIA
MONGOLIA
CHINA
50°
45°
90°
100°
110°
Ophiolitic rocks
Structural grain of basement geology
City
Bayankhongor
N
0km
400km
Russia
Mongolia
China
Kazakh-stan

significance of Central Asian ophiolites and their role in the continental accretion process. Mongolia presents an exceptional opportunity to examine this problem because it lies centrally within the CAOB and contains some of the best-preserved ophiolitic rocks in Central Asia, of which the Bayankhongor ophiolite is the largest (Fig. 1).

The Bayankhongor ophiolite zone (Fig. 1) is situated on the southern side of the Hangai dome that formed during regional Cenozoic uplift (Windley and Allen, 1993; Cunningham, 2001). The ophiolite forms a NW–SE striking sublinear zone, approximately 300-km long and up to 20-km wide (Figs. 1 and 2). Previous mapping enables a four-fold tectonic subdivision of the region from south to north: the Baidrag block, Burd Gol mélange, Bayankhongor zone and Dzag zone (Fig. 2; Teraoka et al., 1996; Buchan et al., 2001).

The Archaean to Palaeoproterozoic Baidrag Block is composed of tonalitic gneiss, granulite and amphibolite, with minor marble and quartzite. A tonalitic gneiss from this block was dated at 2650±30 Ma (U–Pb zircon, Table 1; Mitrofanov et al., 1985), and the block is interpreted as a microcontinent (Mitrofanov et al., 1985; Kozakov et al., 1997).

The Burd Gol mélange (Fig. 2) consists of lenses of sedimentary and igneous rocks enclosed in a matrix of pelite and graphite schists, which are cut by abundant quartz veins. The metamorphic grade increases northwards within the mélange (Buchan et al., 2001). From a palaeontological study of stromatolites in limestone lenses, Mitrofanov et al. (1981) suggested that the Burd Gol mélange is Neoproterozoic in age. Metamorphic white micas within the mélange have ages ranging from 699±35 to 533±3 Ma (Table 1; Teraoka et al., 1996; Höck et al., 2000).

North of the Burd Gol mélange, there is a small area of interbedded marine mudstone and limestone

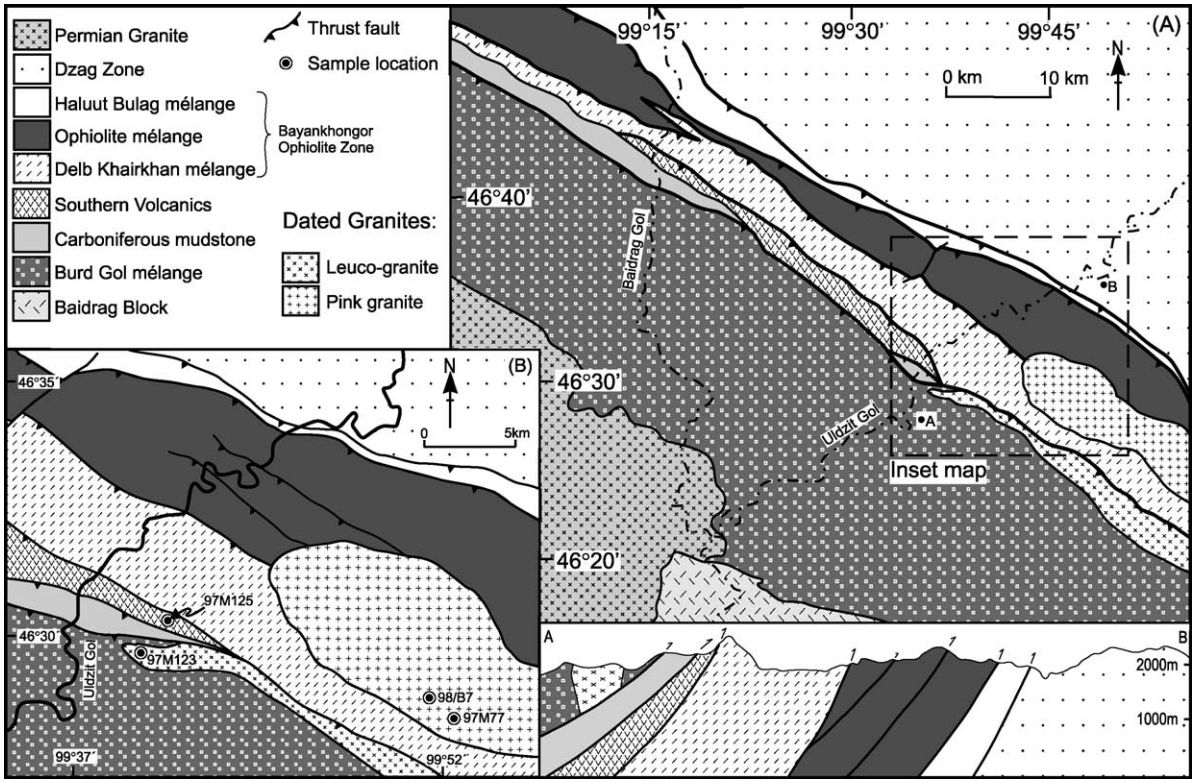

Fig. 2. Regional geology of the Bayankhongor area. Inset map shows detail of study area and sample locations. Location of figure shown in Fig. 1.

Table 1
Summary of isotopic age determinations of lithotectonic units in the Bayankhongor area from past studies

Lithotectonic unit	Age (Ma)	Isotopic method	Mineral analysed	Age interpretation	Location	Source
Dzag	453.9±9.1	K–Ar	white mica	deformation	N46°45.93′E99°26.98′	Kurimoto et al., 1998
Dzag	447.4±9.0	K–Ar	white mica	deformation	N46°19.88′E100°14.50′	Kurimoto et al., 1998
Dzag	395.0±20.0	K–Ar	muscovite	deformation	N46°28.67′E100°11.91′	Teraoka et al., 1996
Dzag	440.0±22.0	K–Ar	muscovite	deformation	N46°32.83′E99°56.65′	Teraoka et al., 1996
Bayankhongor ophiolite	569.0±21.0	Sm–Nd	plag, cpx, amph, whole rock isochron	crystallisation	unknown	Kepezhinskas et al., 1991
Bayankhongor ophiolite	484.5±5.9	Ar–Ar	amphibole	deformation	SE Bayankhongor City	Delor et al., 2000
Burd Gol melange	699.0±35.0	K–Ar	muscovite	deformation	N46°14.84′E99°43.26′	Teraoka et al., 1996
Burd Gol melange	533.0±3.0	Ar–Ar	biotite	deformation	Mount Ushgoeg	Höck et al., 2000
Baidrag block	2650±30	U–Pb	zircon	deformation	N46°15.823′E99°21.335′	Mitrofanov et al., 1985
Palaeozoic granites						
Khangay	249±12	K–Ar	biotite	crystallisation	N47°01.02′E98°33.89′	Oyungerel and Takahashi, 1999
Daltyn-am	247±10	Rb–Sr	whole rock	crystallisation	N46°28.75′E100°02.35′	Oyungerel and Takahashi, 1999
Tsakhyr uul	287±8	Rb–Sr	whole rock	crystallisation	N46°28.75′E100°02.35′	Arakawa et al., 1998
Tsakhyr uul	469±9	K–Ar	biotite	crystallisation	N46°23.6′E99°49.7′	Oyungerel and Takahashi, 1999
Tsakhyr uul	408±20	K–Ar	biotite	crystallisation	N46°23.6′E99°49.7′	Zabotkin, 1988
Tsakhyr uul	451±20	K–Ar	biotite	crystallisation	N46°23.6′E99°49.7′	Zabotkin, 1988
Tsakhyr uul	519	K–Ar	biotite	crystallisation	N46°23.6′E99°49.7′	Andreas, 1970
Tsakhyr uul	551	K–Ar	biotite	crystallisation	N46°23.6′E99°49.7′	Andreas, 1970

that contain Carboniferous fossils (Fig. 2; Dergunov et al., 1997). Between the Carboniferous sedimentary rocks and the Bayankhongor ophiolite zone, there is a thrust-sliver of volcanic rocks (Southern Volcanics in Fig. 2) that Buchan (2002) has shown to have island arc-like geochemical characteristics. The Southern Volcanics have previously been assigned to the Ordovician (Dergunov et al., 1997) or Devonian periods (Tungalag, 1996), based on palaeontological evidence and lithological correlation with similar units elsewhere. Zircons from rhyolite dykes that cross-cut the Southern Volcanics have been dated as part of this study.

The Bayankhongor zone is divided into three subunits: the Delb Khairkhan mélange, ophiolite mélange and the Haluut Bulag mélange (Fig. 2, Buchan et al., 2001). The Delb Khairkhan mélange lies to the south of the ophiolite and contains sedimentary and volcanic rocks of Meso-Neo Proterozoic to Ordovician age enclosed in a matrix of pelitic rocks (Dergunov et al., 1997). The ophiolite mélange contains a complete ophiolite stratigraphy (Moores, 1970), dismembered into blocks enclosed within a serpentinite matrix. Gabbros within the ophiolite mélange have been dated at 569±21 Ma (Sm–Nd cpx–whole rock isochron on gabbro; (Kepezhinskas et al., 1991). Despite a relatively large error range, this age compares well with more precise U–Pb ages for ophiolites along strike to the west (Fig. 1). Metamorphic amphiboles that form lineations within pillow basalts near Bayankhongor City have an age of 484.5±5.9 Ma (Ar–Ar, Table 1.; Delor et al., 2000). The predominantly sedimentary Haluut Bulag mélange contains lenses of bedded limestone, sandstone, siltstone and locally vesicular basalt, enclosed in a matrix of pelitic schist.

The Dzag zone (Fig. 2) consists of asymmetrically folded chlorite–mica schists that contain relict sedimentary features that suggest they are turbidites (Buchan et al., 2001). K–Ar ages (Table 1) for white micas associated with the thrust separating the ophiolite zone and Dzag zone range from 395±20 to

454±9 Ma (Teraoka et al., 1996; Kurimoto et al., 1998).

The structure of the Bayankhongor area is dominated by NW–SE striking, NE directed thrusts, which have juxtaposed the different litho-tectonic units. In addition, the litho-tectonic units have been internally dismembered by sinistral strike-slip displacements, which have contributed to mélange formation. It is unclear whether the strike-slip deformation was a separate event from thrusting, but based on field observations, Buchan et al. (2001) suggest that the two were coeval in a NE-directed transpressive regime.

Buchan et al. (2001) interpreted the Bayankhongor ophiolite as a suture marking the position of an early Palaeozoic subduction zone between the Baidrag block to the south, and the Dzag zone to the north. The Burd Gol mélange represents an accretionary wedge built up against the Baidrag continental block to the south. Subduction was to the southwest, based on the dominant polarity of thrusting within the Bayankhongor ophiolite zone. The ophiolite was obducted in a northeasterly direction over the Dzag zone that represents part of a passive margin to a continent located beneath the sedimentary cover of the Hangai region (Fig. 1).

Several large granite bodies intrude the rocks of the Bayankhongor zone (Fig. 2; Takahashi et al., 1998b); many cut major faults, but are themselves undeformed and so provide useful time constraints on faulting. Takahashi et al. (1998b,c) and Oyungerel (1998) documented the regional petrology, metallogeny and magnetic susceptibility of many of these granites. They suggested that dominantly magnetite-bearing granites occur south of the Dzag zone, whereas dominantly ilmenite-bearing granites occur in the Dzag zone and to the north. Furthermore, they pointed out that this zonation relates to mineralisation, the magnetite-bearing granites being associated with Au–Cu mineralisation, and the ilmenite-bearing granites with Sn–W deposits (Oyungerel, 1998). However, they did not speculate on the relation of the zonation to either source chemistry or tectonic environment of emplacement. Takahashi et al. (1998a) suggested that the zonation also relates to the time of granite emplacement, the ilmenite series being Precambrian–early Palaeozoic, whereas the magnetite series are mostly late Palaeozoic. This interpretation is problematic because most of the dating is based on K–Ar (Oyungerel and Takahashi, 1999) or Rb–Sr ages (Arakawa et al., 1998; Oyungerel and Takahashi, 1999), both of which are easily disturbed during deformation. It is therefore likely that many of these ages are younger than the true crystallisation ages of the granites.

3. Analytical techniques

3.1. Major and trace element geochemistry

Major and trace elements (Table 2) were analysed by XRF at the University of Leicester, using conventional techniques described by Tarney and Marsh (1991). Major elements were measured on fused glass discs using a lithium tetraborate–metaborate flux; trace elements were measured on pressed powder pellets using a Mowiol binding agent. Only major element totals between 98.5% and 101.5% were accepted. For major elements, the typical lower limit of detection (LLD) is 0.01% and precision is better than 0.5% at 100 times LLD. XRF trace element reproducibility is within 5% for international reference materials.

Samples used for REE analysis were digested using microwave digestion in a combined solution of HF–HNO_3. The REE were separated from the bulk sample using Dowex 50W-8X cation-exchange resin. After separation, REE concentrations (Table 2) were determined using an ICP-Optical Emission Spectrometer at the University of Leicester, following the methods described by Harvey et al. (1996). The analytical precision is of the ICP-OES data is ±5%.

3.2. Nd isotope analysis

Nd isotopic compositions (Table 3) were determined using a Finnigan MAT 261 multicollector thermal ion mass spectrometer in static mode at the Max-Planck-Institut für Chemie in Mainz, Germany. Nd isotopic ratios and Nd, Sm concentrations were analysed by isotope dilution using a mixed ^{150}Nd–^{149}Sm spike. The spike was added prior to sample digestion in HF–HNO_3 within closed Teflon™ beakers for >48 h at 200 °C. The REE fraction was

Table 2
Whole rock major and trace element analyses for samples dated in this study

Sample	97M77	97M123	97M125
Lithology	granite	granite	rhyolite dyke
SiO_2	66.49	72.46	70.71
TiO_2	0.51	0.30	0.29
Al_2O_3	15.86	14.69	15.30
Fe_2O_3[a]	3.32	1.97	2.56
MnO	0.07	0.04	0.03
MgO	0.77	0.41	0.12
CaO	1.54	1.73	1.78
Na_2O	4.57	4.39	6.32
K_2O	4.90	4.09	1.51
P_2O_5	0.18	0.12	0.08
LOI	1.27	0.52	2.28
Total	99.46	100.72	100.98
A.S.I	1.02	0.99	1.00
$Temp_{Zrsat}$[b]	814	753	752
Sc	3.7	5.2	3.8
V	35.5	23.2	27.2
Cs	4.2	2.9	2.9
Cu	9.7	1.2	1.0
Mo	1.4	1.6	1.6
Sn	3.0	2.4	2.6
Cr	<1	<1	1.5
Co	8.9	5.7	6.4
Ni	2.4	5.9	2.3
Zn	47.5	40.2	38.8
Ga	19.4	19.3	17.2
Rb	128.3	102.6	31.5
Sr	577.1	585.5	295.5
Y	14.5	10.8	11.7
Zr	254.0	116.6	117.6
Nb	16.9	8.1	3.5
Ba	1403.1	534.4	168.5
Pb	22.2	21.7	4.7
Th	13.5	7.9	4.8
U	2.4	1.7	0.9
La	53.44	17.29	7.86
Ce	103.00	36.03	18.66
Nd	25.63	13.96	10.70
Sm	6.08	3.25	2.47
Eu	1.75	0.84	0.75
Gd	5.25	2.95	2.66
Dy	3.59	2.14	2.13
Er	1.93	1.22	1.14
Yb	1.18	0.96	0.87
Lu	0.24	0.14	0.18
10000*Ga/Al	2.31	2.48	2.12

separated from the bulk sample using Biorad™ 50W-X12 cation-exchange resin. Sm and Nd were separated from the other rare-earth elements using HDEHP-coated Teflon™ powder. Total procedural blanks were <30 pg for Nd. Nd isotopic ratios were normalised to $^{146}Nd/^{144}Nd=0.7219$. Repeated measurements of the La Jolla standard during study and over an extended 6-month period gave $^{143}Nd/^{144}Nd=0.511840\pm0.000036$, $^{145}Nd/^{144}Nd=0.348405\pm0.000022$ and $^{150}Nd/^{144}Nd=0.236480\pm0.000086$ (2σ, n=40).

3.3. Single zircon evaporation technique

Samples were crushed and ground using a jaw crusher and steel disc mill. The ground material was fed over a Rodgers table and heavy minerals were separated from the concentrate using heavy liquids. The resulting heavy mineral concentrate was then fed through a Franz magnetic separator and single zircons were hand-picked from the nonmagnetic fraction.

The evaporation technique, established by Kober (1987), involves repeated evaporation and deposition of Pb isotopes from chemically untreated zircons using a double Re filament arrangement. The laboratory procedures used and comparisons with conventional zircon dating are published in detail elsewhere (Kröner and Todt, 1988). Isotopic measurements were carried out on a Finnigan MAT 261 mass spectrometer at the Max-Planck-Institut für Chemie in Mainz. No correction for mass fractionation was carried out as the effect has been shown to be negligible (Kröner et al., 1999). Measurement of a chip of Curtin University SHRIMP II standard CZ3 yielded a $^{207}Pb/^{206}Pb$ age of 564.8±1.4 Ma, identical to the adopted age of 564 Ma for this standard (Pidgeon et al., 1994).

Internal reproducibility of the evaporation data has been estimated by comparison of conventional U–Pb ages with evaporation ages for fragments of large

Notes to Table 2:
Major elements in wt.%, trace elements in ppm.
LOI=loss on ignition determined at 1050 °C.
A.S.I.=aluminium saturation index (Zen, 1986).
[a] Total iron as Fe_2O_3.
[b] Zircon saturation temperature (Watson and Harrison, 1983).

Table 3
Sm–Nd isotopic data for dated samples

Sample	Lithology	Sm (ppm)	Nd (ppm)	$^{147}Sm/^{144}Nd$	$^{143}Nd/^{144}Nd$ (measured)	$^{143}Nd/^{144}Nd$ (initial)	T_{DM}[a] (in Ma)	T_{DM}[b] (in Ma)	ε_{Nd} (initial)
97M77	Granite	6.08	25.63	0.0867	0.512089±14	0.511783	1270	1350	−3.1
97M123	Granite	3.25	13.96	0.0965	0.512083±19	0.511742	1384	1417	−3.9
97M125	Rhyolite	2.47	10.70	0.1285	0.512622±15	0.512223	943	738	+3.8

Uncertainties for the $^{143}Nd/^{144}Nd$ ratios are 2σ (mean) errors in the last two digits.

ε_{Nd} values are calculated for crystallisation ages given in Table 4 relative to CHUR with present day values of $^{143}Nd/^{144}Nd$=0.512638 and $^{147}Sm/^{144}Nd$=0.1966 (Jacobsen and Wasserburg, 1980). Error is ±0.4 calculated from external reproducibility.

[a] Single-stage Nd Model ages are calculated with a depleted-mantle reservoir and present-day values of $^{143}Nd/^{144}Nd$=0.513151 and $^{147}Sm/^{144}Nd$=0.214 (Goldstein et al., 1984).

[b] Two-stage model age following method of DePaolo et al. (1991) assumes average upper crustal evolution (1st stage) of source until time of crystallisation of granite. Thereafter, evolution is calculated using measured values (2nd stage).

grains from the Phalaborwa Complex, South Africa. These zircons, used as a laboratory standard, are euhedral, colourless to slightly pink and completely homogenous when examined under cathodoluminescence. Conventional U–Pb analyses of six separate grain fragments from this sample yielded a $^{207}Pb/^{206}Pb$ age of 2052.2±0.8 Ma (2σ)(W. Todt, unpublished data), whereas the mean $^{207}Pb/^{206}Pb$ ratio for 18 grains, evaporated individually over a period of 12 months, is 0.126634±0.000026 (2σ error of the population), corresponding to an age of 2051.8±0.4 Ma, identical to the U–Pb age.

Table 4
$^{207}Pb/^{206}Pb$ isotopic age data from zircon evaporation

Sample no.	Location	Zircon colour and morphology	Measurement no.	Number of grains	Mass scans[a]	Evaporation temperature (°C)	Mean $^{207}Pb/^{206}Pb$ ratio[b] and 2σ (mean) error	$^{207}Pb/^{206}Pb$ age and 2σ (mean) error (Ma)
97M77 (a)	N46°26.360′ E99°52.044′	Prismatic, clear to light pink, idiomorphic	Single	3	136	1601	**0.058405±315**	**545±2**
97M77 (b)		Short-prismatic, clear to yellow, idiomorphic, rounded ends	1	3	79	1598	0.060377±317	617±11
			2	4	39	1598	0.060122±238	608±9
			3	2	37	1595	0.060283±125	614±5
			1–3		155		0.060290±175	614±6
97M77 (c)		Long-slightly rounded ends, pink, idiomorphic	Single	3	80	1598	0.068214±87	875±3
97M123	N46°30.022′ E99°38.251′	Long-prismatic, needle-like, clear, idiomorphic	1	4	67	1595	0.058240±206	539±8
			2	7	37	1570	0.058194±211	541±8
			3	5	18	1598	0.058114±266	534±10
			1–3		122		**0.058238±136**	**539±5**
97M125 (a)	N46°31.307′ E99°39.346′	Short prismatic, clear to pink, idiomorphic	Single	4	65	1603	**0.056551±213**	**474±8**
97M125 (b)		Pink to brown, idiomorphic	Single	2	121	1550	0.097548±122	1578±2
M98/B7	N46°26.538′ E99°51.229′	Clear to yellow-brown, long-prismatic, idiomorphic to slightly rounded	1	Single	88	1599	0.058238±38	534±1
			2	Single	77	1598	0.058229±43	538±2
			3	Single	88	1595	0.058226±41	538±2
			4	Single	88	1597	0.058272±37	540±1
			1–4		341		**0.058242±20**	**539±1**

See Fig. 2 for sample location; ages in bold type are interpreted crystallisation ages of the sample.

[a] Number of $^{207}Pb/^{206}Pb$ ratios evaluated for age assessment.

[b] Observed mean ratio corrected for nonradiogenic Pb where necessary. Errors based on uncertainties in counting statistics.

Table 4 lists the calculated $^{207}Pb/^{206}Pb$ ratios and errors that are the weighted means of all measurements. The $^{207}Pb/^{206}Pb$ spectra are shown in histograms (Figs. 6–9) to permit visual assessment of the data distribution from which the ages are derived. Since the evaporation technique only provides Pb isotope ratios, there is no a priori way to determine whether a measured $^{207}Pb/^{206}Pb$ ratio represents a concordant age. Thus, in principle, all $^{207}Pb/^{206}Pb$ ages determined by this method are necessarily of minimum ages. However, a number of studies have shown that there is a strong likelihood that these data represent crystallisation ages when: (a) the $^{207}Pb/^{206}Pb$ ratio does not change appreciably with increasing temperature of evaporation; and/or (b) repeated analysis of grains from the same sample at high evaporation temperatures yields the same isotopic ratios within error.

The rationale behind this is that it is highly unlikely that each grain in a zircon population has lost exactly the same amount of Pb, and therefore that grains with Pb loss would yield highly variable $^{207}Pb/^{206}Pb$ ratios and ages. Comparative studies using single zircon evaporation, conventional U–Pb dating and ion-microprobe analysis have shown that this is correct (e.g. Kröner et al., 1991; Cocherie et al., 1992).

4. Petrography, geochemistry and zircon geochronology

4.1. Sample 97M123—leucogranite

Sample 97M123 was taken from a leucocratic granite pluton, which intrudes the Burd Gol mélange approximately 1 km east of Uldzit Gol (Fig. 2), and forms part of the Tsakhir Uul granite complex (Oyungerel, 1998). The granite appears to have been emplaced along a thrust fault that separates the Burd Gol mélange from Carboniferous rocks to the north. A weak foliation is developed on the northern margin of the granite along the thrust fault, but is only found over a width of a few metres.

4.1.1. Petrography

97M123 is a medium to coarse-grained biotite-bearing leucogranite. Large (5 mm) phenocrysts of zoned plagioclase, microperthite and quartz are enclosed in an interlocking matrix of finer-grained plagioclase, orthoclase, rare microcline and quartz. The plagioclase phenocrysts have been slightly resorbed around their edges suggesting a possible xenocrystic origin. Rare graphic intergrowths of quartz and potassium feldspar occur in the matrix. Biotite forms anhedral, randomly orientated laths around 2–3 mm in length; muscovite is rare. Zircon and apatite are the main accessory phases and opaques are minor. The bulk of the rock is very fresh, but some of the larger plagioclase phenocrysts have altered cores in which sericite and epidote have replaced plagioclase.

4.1.2. Geochemistry

Sample 97M123 has the highest SiO_2 (72.46 wt.%) concentration of the dated samples, but has similar Na_2O (4.39 wt.%) and K_2O (4.09 wt.%) concentrations to the pink granite sample 97M77 and a CaO (1.73 wt.%) concentration close to that of the rhyolite sample 97M125 (Table 2). It has an aluminium saturation index (A.S.I.)=0.99 (Zen, 1986; Table 2), which indicates that the leucogranite is slightly metaluminous (Fig. 3). Primitive mantle normalised trace element patterns (Fig. 4) indicate enrichment in LILE (e.g. Rb=102.6 ppm, Ba=534.4 ppm) and selective enrichment of HFSE such as Th (7.9 ppm) and Zr (116.6 ppm), but depletion of others indicated by negative Nb (Nb/La_{PRIMA}=0.47) and Ti (Ti/Zr_{PRIMA}=0.14) anomalies. Chondrite normalised REE patterns (Fig. 5) indicate enrichment of LREE relative to HREE (La/Yb_{chnd}=12.9). These trace and rare-earth element characteristics are typical of average upper continental crust patterns (Plank and Langmuir, 1998; Barth et al., 2000). Measured Nd isotopic compositions give a calculated initial $\varepsilon_{Nd(539)}=-3.9$, and two-stage depleted mantle model age of 1417 Ma (Table 3; DePaolo et al., 1991).

4.1.3. Geochronology

All zircons from sample 97M123 are transparent, euhedral, prismatic, needle-like crystals that have magmatic morphologies (Fig. 6). Because the zircons are small, approximately 50–120 μm in length, several grains were analysed together (Table 4). The measurements were repeated three times with a different number of zircons each time in order to check that the number of grains did not affect the measured

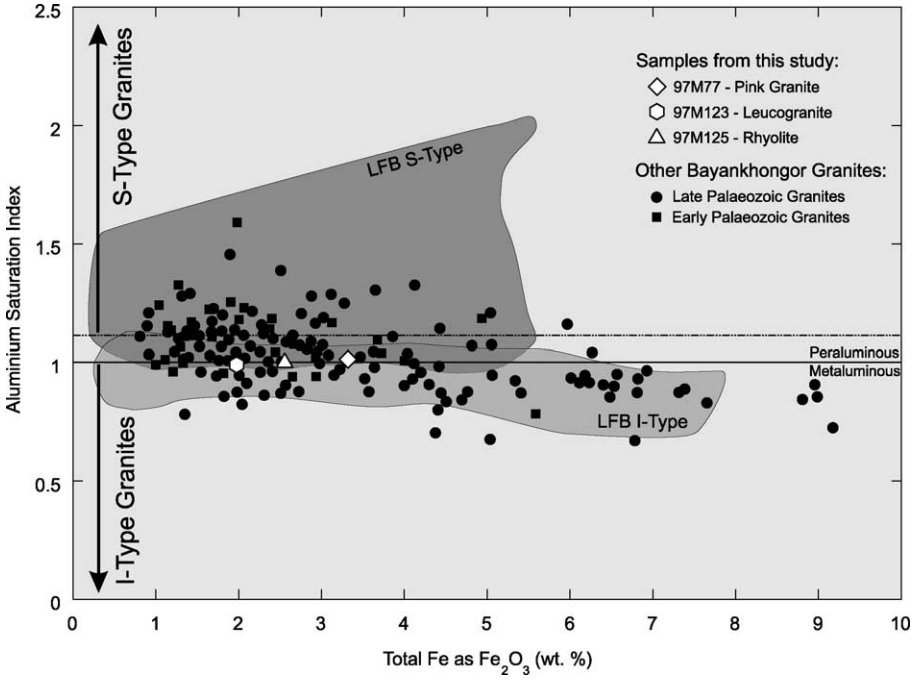

Fig. 3. Aluminium saturation index vs. total Fe demonstrating the dominantly transitional nature between S-type and I-type granites in the Bayankhongor area. S- and I-type fields after Blevin and Chappell (1995), additional Palaeozoic granite data from Takahashi et al. (1998b).

ratios (Fig. 6, Table 4). Three repeat measurements yielded consistent $^{207}Pb/^{206}Pb$ ratios with a mean of $^{207}Pb/^{206}Pb=0.058238\pm136$, corresponding to an age of 539±5 Ma (Fig. 6, Table 4). This age is interpreted to reflect the time of crystallisation of the leucogranite.

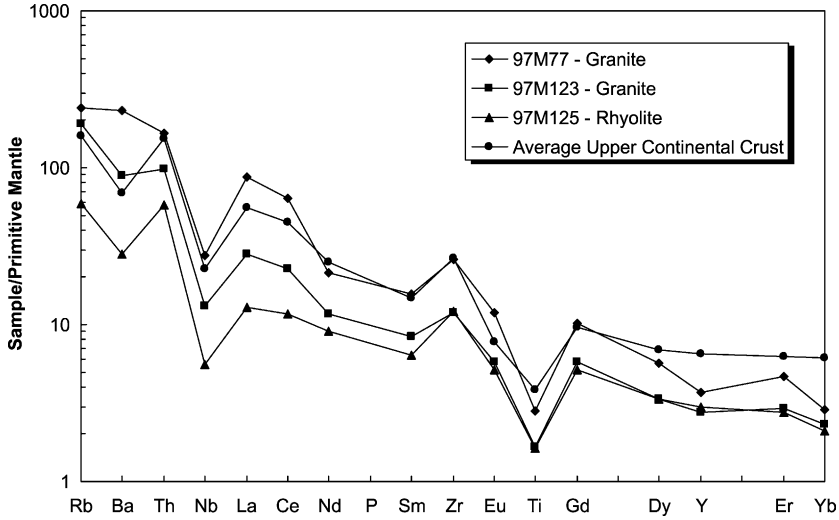

Fig. 4. Trace element patterns of dated samples normalised to PRIMA. Patterns for studied rocks are similar to those for average upper continental crust (Plank and Langmuir, 1998; Barth et al., 2000). Average upper continental crust composition is based on a combination of published data from Plank and Langmuir (1998) and Barth et al. (2000). PRIMA normalisation data from Hofmann (1988).

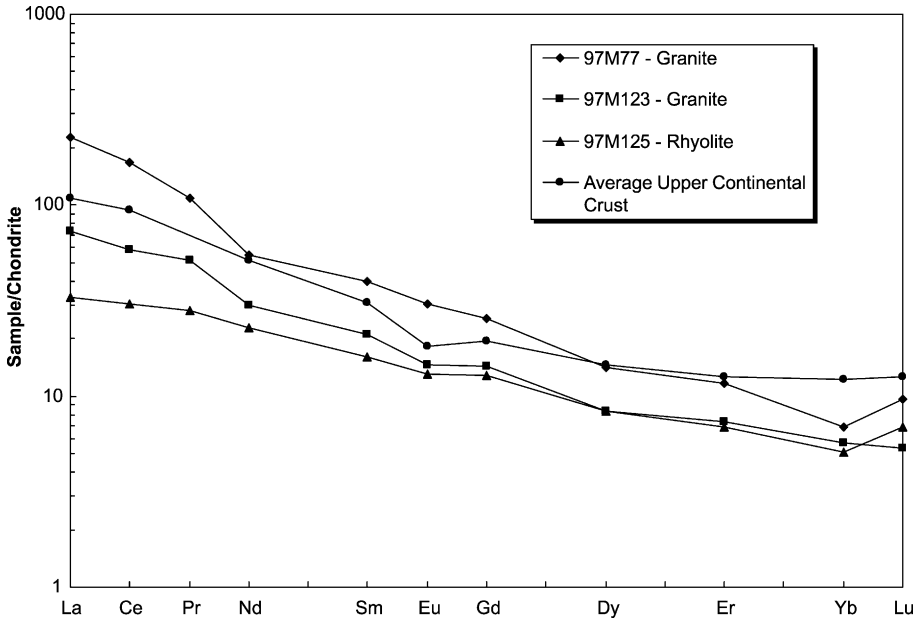

Fig. 5. Chondrite normalised REE patterns for dated samples have similar trends to average upper continental crust (Plank and Langmuir, 1998; Barth et al., 2000). Average upper continental crust composition is based on a combination of published data from Plank and Langmuir (1998) and Barth et al. (2000). Normalisation data from Sun and McDonough (1989).

4.2. Sample 97M77 and M98/B7—granite

Samples 97M77 and M98/B7 were collected from different locations within the same, previously unmapped, granite intrusion approximately 15 km southeast of Uldzit Gol (Fig. 2). This undeformed granite has intruded the Delb Khairkhan mélange and the ophiolite mélange, and cuts the thrust fault separating them, as well as other internal faults within the mélanges (Fig. 2).

4.2.1. Petrography

Both samples are medium-grained (≤5 mm) biotite-bearing pink granites. The grain size in the pluton varies with some very coarse-grained areas containing feldspar crystals up to 6–10 cm in length. The samples are roughly equigranular with quartz, plagioclase, microcline, microperthite and orthoclase forming a matrix of intergrown crystals with consertal texture. Local graphic intergrowths of quartz and potassium feldspar are also present. Biotite forms 2–5 mm laths, which are almost totally altered to chlorite. Plagioclase and some potassium feldspars are also heavily altered to sericite and clay minerals. Iron oxide-rich veins cut the samples, but they are only a few millimetres wide. Sphene and zircon are the dominant accessory phases, and apatite and opaques are minor.

4.2.2. Geochemistry

Because samples 97M77 and M98/B7 were taken from the same granite, only sample 97M77 was chemically analysed. Sample 97M77 has the lowest SiO_2 (66.5 wt.%) and CaO (1.54 wt.%) compositions of the dated samples, but has similar Na_2O (4.57 wt.%) and K_2O (4.9 wt.%) concentrations to the leucogranite sample 97M123 (Table 2). Its A.S.I.=1.02 (Table 2) is the highest of the analysed samples and suggests that it is slightly peraluminous (Fig. 3). Primitive mantle normalised trace-element patterns (Fig. 4) indicate enrichment in LILE (e.g. Rb=128.3 ppm and Ba=1403.1 ppm) and selective enrichment of HFSE such as Th (13.5 ppm) and Zr (254.0 ppm), but depletion in Nb and Ti, indicated by marked negative anomalies in Fig. 4 (Nb/La_{PRIMA}=0.32, Ti/Zr_{PRIMA}=0.11) as was the case for the leucogranite. Chondrite normalised REE patterns (Fig. 5) show enrichment of LREE relative to HREE (La/Yb_{chnd}=32.5). Sample

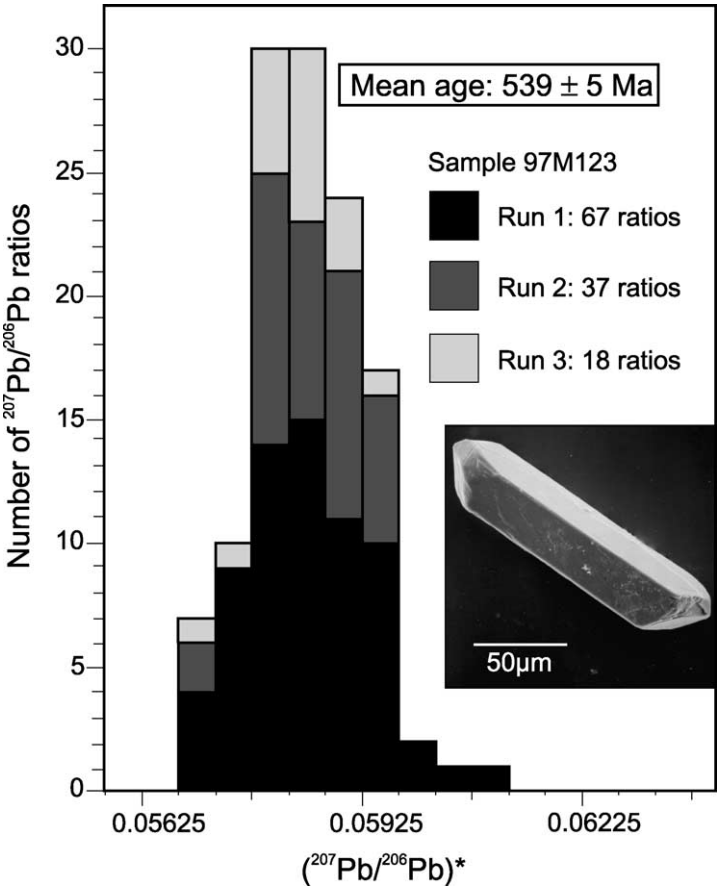

Fig. 6. Histogram of measured $^{207}Pb/^{206}Pb$ ratios for sample 97M123.

97M77 has similar Nd isotopic characteristics to 97M123 with an initial $\varepsilon_{Nd\ (545)}=-3.1$ and a two-stage depleted mantle model age of 1350 Ma (Table 3; DePaolo et al., 1991).

4.2.3. Geochronology

4.2.3.1. Sample M98/B7. Zircons from M98/B7 are prismatic, clear to yellow-brown and idiomorphic to slightly rounded. The grains are relatively large, approximately 150–200 μm in length, compared with other populations and thus were analysed as single grains. The experiments were repeated four times with separate single grains to confirm the calculated age. The $^{207}Pb/^{206}Pb$ ratios from each run were consistent with a mean value of $^{207}Pb/^{206}Pb=0.058242\pm20$ (Table 4) corresponding to an age of 539±1 Ma (Fig. 7). This age most likely represents the time of crystallisation of the granite.

4.2.3.2. Sample 97M77. There are three different populations of zircons in this sample (97M77 a–c, Table 4) that were each analysed separately. Population (a) is similar to the M98/B7 zircons: prismatic, clear to light pink and idiomorphic (Fig. 8a). However, the grains in 97M77 are smaller (approximately 60 μm), so three grains were analysed together to ensure a strong signal during measurement. The measured mean $^{207}Pb/^{206}Pb=0.058405\pm315$ ratio corresponds to an age of 545±2 Ma (Fig. 8a, Table 4). Only one experiment was done for this population, and 136 mass scans were collected while the evaporation temperature was as high as 1601 °C, ensuring that the grains were completely evaporated. In addi-

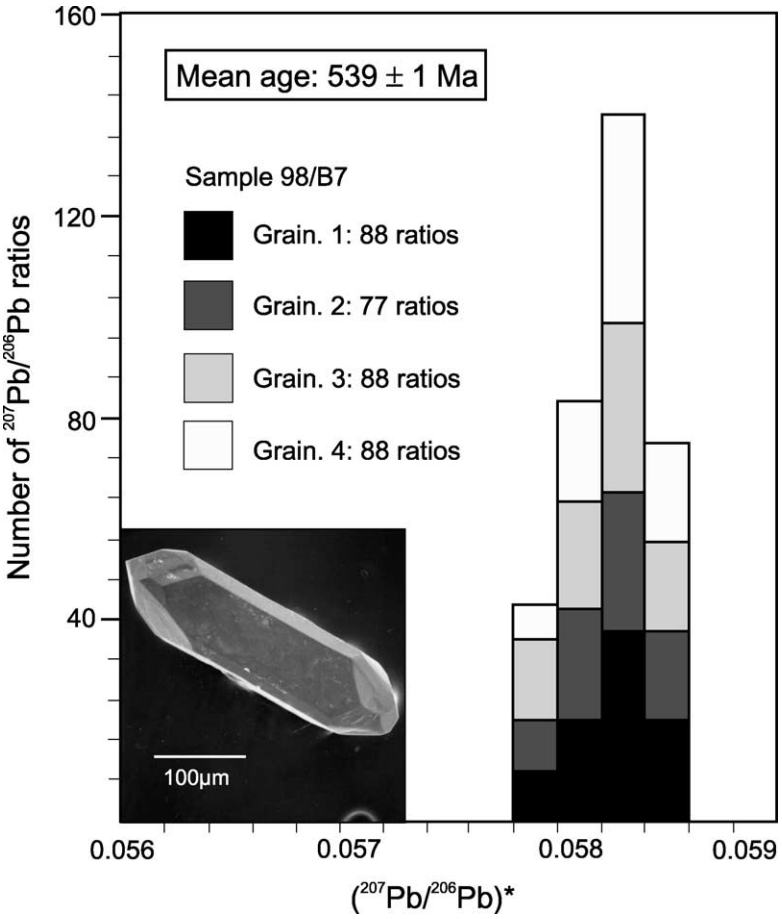

Fig. 7. Histogram of measured $^{207}Pb/^{206}Pb$ ratios for sample M98/B7.

tion, the determined age compares well with that of M98/B7, which had similar population morphology and is from the same granite pluton.

Population (b) consists of short prismatic zircons that are clear to yellow and have slightly rounded terminations (Fig. 8b). The grains are small, <100 μm in length, and so several grains were analysed together. Three repeat measurements yielded mean $^{207}Pb/^{206}Pb$ ratios of $^{207}Pb/^{206}Pb=0.060290\pm175$ corresponding to an age of 614±6 Ma (Table 4; Fig. 8b).

Population (c) contains long, thin, pink, prismatic grains with rounded ends (Fig. 8c). They are about 80 μm in length and so several grains were therefore analysed together (Table 4). A single experiment for this population with 80 isotopic ratios produced a mean ratio of $^{207}Pb/^{206}Pb=0.068214\pm87$, which correspond to an age of 875±3 Ma (Fig. 8c; Table 4).

Because the morphology of population (a) suggests that the zircons are magmatic and the age is similar to that of M98/B7, we interpret this as the crystallisation age of the granite. Despite slightly rounding of the ends of zircons in populations (b) and (c), they clearly have magmatic morphology (Fig. 8) and are interpreted as inherited zircons from an older source rock.

4.3. Sample 97M125—rhyolite

This sample was collected from a swarm of rhyolite dykes that intrude the Southern Volcanics approximately 2 km east of the Uldzit Gol (Fig. 2). The dykes trend dominantly NE and are confined to the

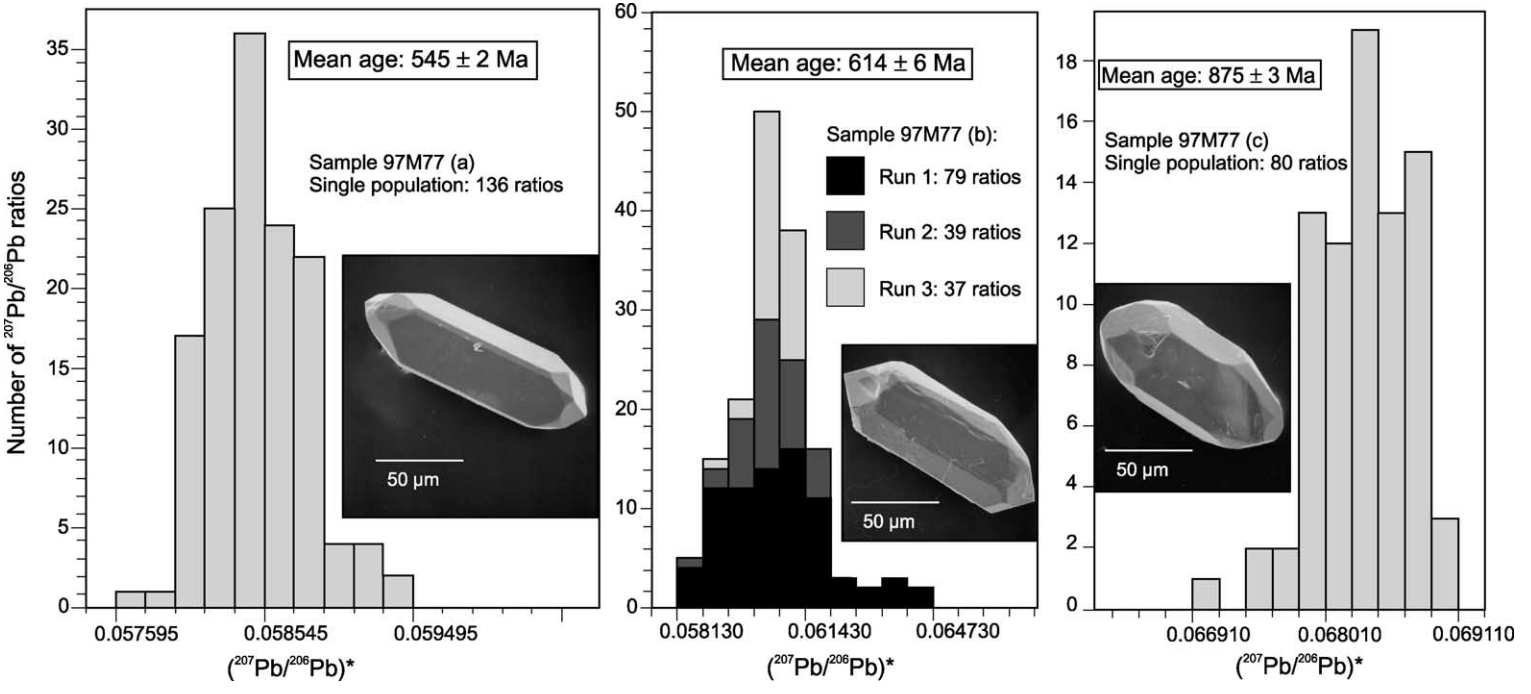

Fig. 8. Histograms of measured $^{207}Pb/^{206}Pb$ ratios for three morphologically distinct zircon populations in sample 97M77. See Table 4 for morphological description.

volcanic unit because none are found in either the Carboniferous rocks to the south or the Delb Khairkhan mélange to the north. The dykes have highly irregular contacts with the surrounding volcanic rocks and in places contain volcanic xenoliths.

4.3.1. Petrography

A single 3m wide dyke was sampled. The sample contains 0.3–0.5 mm quartz, potassium feldspar and plagioclase phenocrysts and some larger plagioclase glomerocrysts, enclosed in a matrix of finer grained, randomly orientated quartz and plagioclase. The plagioclase phenocrysts are altered to sericite and epidote. Some quartz phenocrysts have irregular rounded margins and are slightly resorbed. The groundmass contains a small amount of fine-grained (<0.1 mm) anhedral muscovite. Sphene and opaques are the dominant accessory phases, but apatite and zircon are also present. Calcite and hematite veins cut the sample, but are generally less than a millimetre wide.

4.3.2. Geochemistry

Sample 97M125 has a similar SiO_2 (70.71 wt.%) and CaO (1.78 wt.%) concentration to the leucogranite sample 97M123. However, it has the highest Na_2O (6.32 wt.%) and lowest K_2O (1.51 wt.%) concentration of the samples analysed in this study. Its A.S.I.=1.00 (Table 2) lies on the boundary between peraluminous and metaluminous granites (Fig. 3). Primitive mantle normalised trace element patterns (Fig. 4) indicate enrichment in LILE (e.g. Rb=31.4 ppm, Ba=168.5 ppm) and selective enrichment of HFSE (e.g. Th=4.8 ppm and Zr=117.6 ppm), but depletion of others indicated by negative Nb (Nb/La_{PRIMA}=0.44) and Ti (Ti/Zr_{PRIMA}=0.13) anomalies, similar to the other dated samples. However, sample 97M125 has a generally lower concentration of trace elements than either 97M123 or 97M77 (Fig. 4, Table 2). Chondrite normalised REE patterns (Fig. 5) indicate that 97M125 is enriched in LREE relative to HREE (La/Yb_{chnd}=6.48). The Nd isotopic concentra-

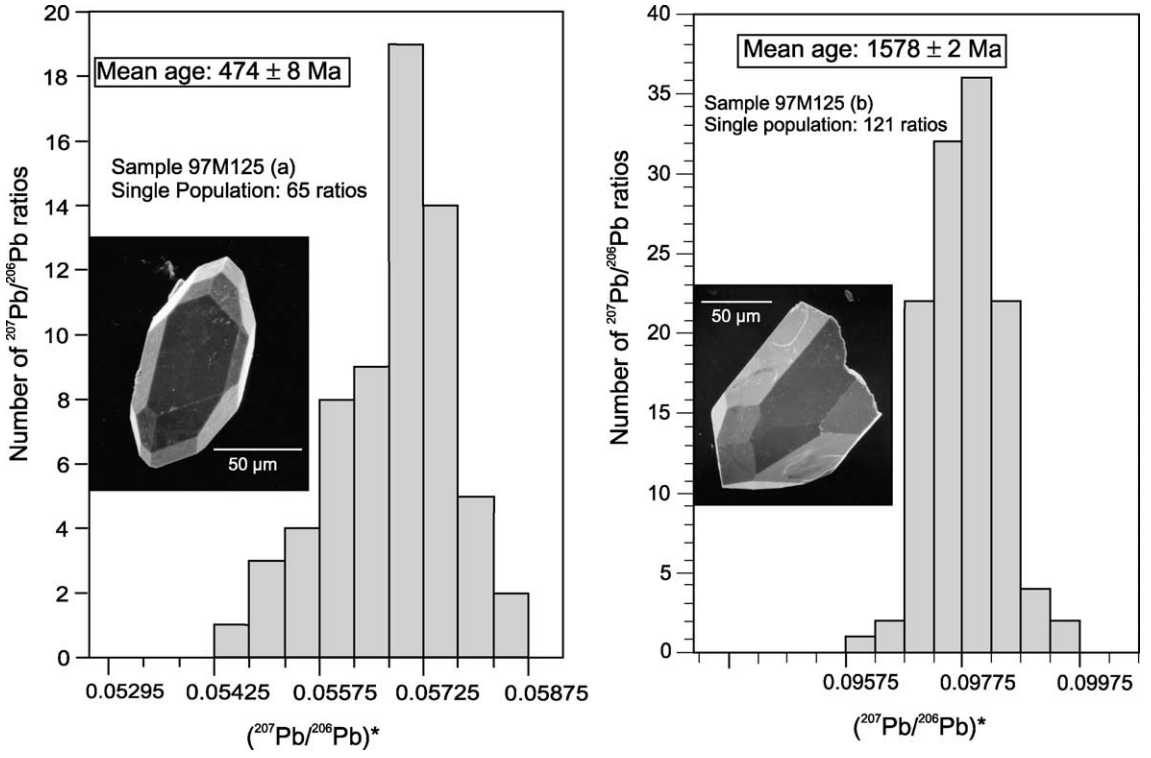

Fig. 9. Histogram of measured $^{207}Pb/^{206}Pb$ ratios for two morphologically distinct zircon populations in sample 97M125. See Table 4 for morphological description. The crystallisation age of 474 Ma provides a minimum age in the Ordovician for the Southern Volcanic unit that they intrude, which has previously been assigned to either the Devonian (Tungalag, 1996) or Ordovician (Dergunov et al., 1997) periods.

tion of sample 97M125 is very different from samples 97M123 and 97M77, sample 97M125 has an initial ε_{Nd}=+3.8 and a two-stage depleted mantle model age of 738 Ma, which is around 750–800 Ma younger than 97M123 and 97M77 (Table 3).

4.3.3. Geochronology

Sample 97M125 contains two zircon populations (a) and (b) shown in Table 4. Population (a) contains zircons that are short, idiomorphic, prismatic and clear to pink (Fig. 9a). The crystals are small, between 50 and 100 μm in length, and so four grains were analysed simultaneously to ensure a strong signal during measurement. The measured mean $^{207}Pb/^{206}Pb$=0.056551±213 (Table 4) corresponds to an age of 474±8 Ma (Table 4; Fig. 9a).

Population (b) contains idiomorphic, slightly pink to brown, broken zircons (Fig. 9b). The fragments are approximately 80–100 μm in size, suggesting that the original zircons were large compared to the populations from other samples in this study. The measured mean $^{207}Pb/^{206}Pb$=0.097548±122 corresponds to an age of 1578±2 Ma (Table 4; Fig. 9b), making this the oldest population analysed in this study.

The zircon morphology suggests that population (a) is of magmatic origin and the age of 474 Ma is interpreted to reflect the time of crystallisation of the rhyolite dykes. The large broken zircons of population (b) do not appear to have been abraded in any way as the terminations of the fragments are not noticeably rounded and, therefore, it appears that these are also magmatic. The older age of population (b) means that it must be interpreted as an inherited population from the melt source(s).

5. Discussion

Interpretations of the structural and lithological characteristics of the Bayankhongor Zone suggest that the major lithotectonic units were amalgamated by a mechanism of subduction–accretion (Buchan et al., 2001). The analysed granites and rhyolite dykes intrude the accreted blocks and so provide important constraints on the relative timing of accretion and the duration of subduction and collision. The new data indicate that there were at least two Palaeozoic granite-forming events at c. 540 and 474 Ma. An important consideration is whether the granite magmas were produced during collisional accretionary processes, or by subduction prior to accretion.

5.1. Magma sources and tectonic setting

The limited chemical database of just three samples in this study makes it difficult to draw firm conclusions on the nature of magma source components and the emplacement environment. However, by combining these data with those from previous studies of granites in the Bayankhongor area (e.g. Takahashi et al., 1998a,b), and of the rocks that the granites and rhyolite dykes intruded (e.g. Buchan et al., 2001), we can establish some important constraints.

Central Asia contains many large A-type granite plutons that were intruded during the Palaeozoic, predominantly in the Permian (Jahn et al., 2000). It is therefore important to determine whether the granites analysed in this study reflect A-type magmatism, which would define a specific tectonic environment for their emplacement. Whalen et al. (1987) defined a chemical discrimination to separate A-type granites from the I- and S-type granites of Chappell and White (1992), based on the ratio of Ga/Al in the granite that can be plotted against several trace and major elements that tend to be concentrated in A-type granites. One commonly used is Ga/Al versus Y in which an A-type granite is determined to have a 10000 Ga/Al ratio >2.6 and a concentration of Y>80 ppm. Any granite with a value below this is deemed either an I- or S-type. The granites in this study have 10000 Ga/Al=2.1–2.4 and Y concentrations between 10.8 and 14.5 ppm (Table 2), which suggests that they are not A-type granites. In addition, the Permian A type granites are characterised by positive ε_{Nd} values, which are interpreted to suggest that these granites were derived from a direct mantle melt with no crustal addition (Jahn et al., 2000), whereas the granites in this study have negative ε_{Nd} values, suggesting a magma source containing an older more enriched component, typically assumed to be continental crust.

Chappell and White (1992) define S type granites as only peraluminous (A.S.I.>1.1, Fig. 3), due to concentration of Al in clay minerals during chemical weathering of sedimentary source rocks, and I type as generally metaluminous to mildly peraluminous (A.S.I.<1.0, Fig. 3) because their igneous source rocks

have not inherited the same weathering products. All three dated rocks in this study have major element characteristics that indicate they are compositionally transitional between metaluminous and peraluminous granites (i.e. A.S.I. between 0.99 and 1.02; Fig. 3) and are therefore transitional between I-type and S-type granites. Our data combined with that of Takahashi et al. (1998a,b; Fig. 3) indicate that these compositional characteristic are shared by the majority of Palaeozoic granites found in the Bayankhongor Zone. This is not surprising because the greater part of the Bayankhongor area is composed of mélanges containing both igneous (dominantly mafic) and sedimentary lithologies (Buchan et al., 2001). Therefore, even if the magma source in the deep crust was relatively homogenous, the rising magma could acquire transitional characteristics by assimilating some of the wall rocks into the magma. As different magma bodies would have passed through mélanges with varying proportions of igneous and sedimentary material, they could correspondingly assimilate different quantities of each and become more peraluminous or metaluminous. This is probably the most likely explanation for the spread of data in Fig. 3.

Despite the apparent similarities in source chemistry of Bayankhongor granites, the Sm–Nd isotopic characteristics of the studied samples reveal some marked differences. Granite samples 97M123 and 97M77 have enriched source characteristics indicated by an initial $\varepsilon_{Nd\ (540)} \approx -3$ (Table 3), whereas the rhyolite sample 97M125 has an initial $\varepsilon_{Nd\ (474)} = +3.8$ (Table 3), indicating a moderately depleted source. Recalculating ε_{Nd} of the granite samples to the crystallisation age of the rhyolite dyke at 474 Ma gives $\varepsilon_{Nd\ (474)} = -4.8$ for the leucogranite (97M123) and $\varepsilon_{Nd\ (474)} = -4.1$ (97M77), indicating that the granites and rhyolite dykes must have different source components, or at least a different mixture of components.

There are three scenarios that could account for these differences in source characteristics. The first and perhaps the more obvious is that the rhyolite dykes were emplaced 70 Ma after the granites and, therefore, different sources were available at the different times as the accretionary complex developed. Alternatively, consideration of the field relations of the Southern Volcanic rocks shows that they are completely fault bounded except where they come into contact with the younger Carboniferous sedimentary rocks (Fig. 2). This suggests that the Southern Volcanics may have been juxtaposed with the rest of the Bayankhongor units after the rhyolite dykes were emplaced. Indeed, the rhyolites may have been an integral part of the volcanism. Late juxtaposition would also account for the fact that the volcanic rocks are less intensely deformed than surrounding units and that the rhyolite dykes are confined within the Southern Volcanics (Buchan et al., 2001).

Both of the above suggestions are complicated by spatial relationships and timing of deformation, but are possible due to the tectonic complexity of subduction–accretion environments. However, the final scenario does not require large movements of the volcanic rocks in order to account for differences in source chemistry. The multiple zircon populations of 97M77 and 97M125 (Table 4) indicate that older rocks were at least partially assimilated into the magma. Therefore, just as the mixed lithologies in the mélanges could be responsible for the similarities in major element chemistry, it could also account for the differences in isotopic chemistry. If it is assumed that the major thrust units in the Bayankhongor zone are continuous to depth, then it is probable that the two granites have sampled most of the same lithologies and therefore have comparable chemical and isotopic characteristics. However, the rhyolite dykes were intruded solely into the Southern Volcanic rocks, fragments of which are found as partially resorbed xenoliths within the dykes. Therefore, the volcanic rocks may be responsible for the difference in isotope chemistry. Also, the fact that there are only dykes and no larger intrusive bodies of this age may suggest that this was a relatively small partial melt fraction that would be more easily susceptible to changes in isotopic composition due to mixing. However, this could also reflect a problem of sampling over a small area. The inherited zircon population in the rhyolite (97M125) is an important factor in the mixing scenario because its age of 1578±2 Ma (Table 4) is comparable to the Nd model age of the granite samples (1417 Ma, Table 3), taking into account mixing of younger rocks with the granite magma, suggesting that the same source may have contributed in part to the rhyolite magma. At present, it is difficult to resolve these questions because the tectonic relationship of the Southern Volcanics to the rest of the

Bayankhongor units is not completely understood; i.e. it is unclear whether the volcanics were built on top of the Burd Gol accretionary complex (Fig. 2) during subduction of the Bayankhongor ophiolite crust, or whether they represent part of a separate island arc that was later juxtaposed (Buchan et al., 2002).

However, the following constraints on the possible sources of the granites and rhyolite dykes can be suggested. Both granite samples (97M77 and 97M123) crystallised from a melt extracted from an enriched source that has a minimum crustal-residence age (O'Nions et al., 1983) of between 1350 and 1417 Ma based on two-stage Nd model ages (Table 3). It is likely that the actual time of crust–mantle differentiation of the granite magma source was significantly older and more enriched than the granite magma (i.e. had a more negative ε_{Nd} value), because the chemical and isotopic characteristics of the magma were modified by assimilation of younger crust as indicated by the inherited zircon populations of 97M77 and the general transitional character between I-type and S-type granite (Arndt and Goldstein, 1987).

Therefore, the most likely sources would be either sediments produced by erosion of old continental crust or the continental crust itself. Buchan et al. (2001) suggest that the Bayankhongor ophiolite was obducted onto the Dzag Zone (Fig. 2), which represents the passive margin of a continent that lies beneath the Hangai region (Fig. 1). The ophiolite was later deformed during the collision and suturing of the Baidrag block and the Hangai continent. Granite occurrences are common in collisional settings where sediments or quartz–feldspathic continental basement is melted due to increased pressure and temperature on burial by thrust stacking. Therefore, the Hangai continent and original passive margin sedimentary cover are strong candidates for the granite source. Unfortunately, the proposed Hangai continent is not exposed in the study area and so there are no data on its chemical and isotopic characteristics. Nevertheless, a comprehensive study of depleted mantle model ages from granites in the Hangai region by Kovalenko et al. (1996b) identified several bodies with model ages in the range 1200–1600 Ma similar to those determined for the two granites of this study. Because of the depleted magma signature (ε_{Nd}=+3.8) of the rhyolites and much younger depleted mantle model age (943 Ma single-stage, 738 Ma two-stage), it is unlikely that the main magma source of the rhyolite was the same continental material. For example, in order to achieve a depleted magma positive ε_{Nd} signature from a bulk melt that was initially enriched (negative ε_{Nd}) would require assimilation of large amounts of depleted oceanic and/or island arc volcanic rocks because the very low concentrations of Nd in these rocks would have little effect on the overall magma concentrations. Conversely, a small amount of an enriched melt mixed with an initially depleted melt could easily cause the resultant magma to have more enriched characteristics due to high concentrations of Nd in these rocks relative to the depleted magma. Therefore, it is more likely that the initial rhyolite magma was more depleted (for example a depleted mantle melt at 474 Ma would be expected to have an initial $\varepsilon_{Nd\ (474)} \approx +8.9$) and that a small amount of continental basement or sediment was mixed with the magma resulting in a less depleted ε_{Nd} value and older model age. This would also be consistent with the inherited zircon population found in the rhyolite with an age of 1577 Ma, which requires an older crust component.

Field evidence of a contractional or transpressional regime throughout the Palaeozoic (Buchan et al., 2001), combined with the chemical and isotopic characteristics of the granite samples 97M77 and 97M123, strongly supports a collisional setting for granite generation. The zircon saturation temperatures determined for the samples are between 750 and 800 °C (Table 2), which are within the range that Thompson (1999) suggests are obtainable during collisional burial resulting in high degrees of melting. Therefore, it seems most likely that the granites were emplaced during collision of the Bayankhongor ophiolite and Burd Gol mélange with the Dzag zone and Hangai continent, and that the rocks of the Hangai continental crust and/or the Dzag passive margin were the main magma source. The rhyolite dykes may also have been produced during this collision or they might represent a fragment of an allochthonous arc that was later juxtaposed by faulting.

5.2. Emplacement timing and the tectonic history of the Bayankhongor Ophiolite Zone

Having considered the possible magma source components of the granites and rhyolite dykes and

established that they were likely produced during terrane collision, it is now possible to examine the constraints that our ages provide for the timing and duration of deformation within the Bayankhongor accretionary system. The pink granite (97M77) and leucogranite (97M123) provide constraints on the deformation in the Bayankhongor ophiolite zone and the Burd Gol mélange. The pink granite (97M77 and M98/B7) cross-cuts the thrust fault that juxtaposes the ophiolitic rocks with the Delb Khairkhan mélange, as well as several smaller internal faults within the ophiolite mélange (Fig. 2). The pink granite itself is not deformed, which suggests that none of these faults moved significantly after intrusion. This provides constraints on the timing of obduction of the ophiolite rocks, as they must have been in place before intrusion of the pink granite at 544 Ma. In addition, the whole ophiolite zone including the Delb Khairkhan mélange must have collided or been accreted to the Burd Gol accretionary complex by 539 Ma, because the leucogranite has the same crystallisation age and so it can be assumed that it was produced by the same or coeval event. If the Hangai continent and/or Dzag passive margin were the source for the granite magmas, then these units must also have at least begun colliding with the ophiolite and accretionary complex by 544 Ma. The ophiolite is interpreted to have formed at 569±21 Ma (Kepezhinskas et al., 1991; Table 1), which suggests a period of approximately 25–30 Ma between formation and closure of the

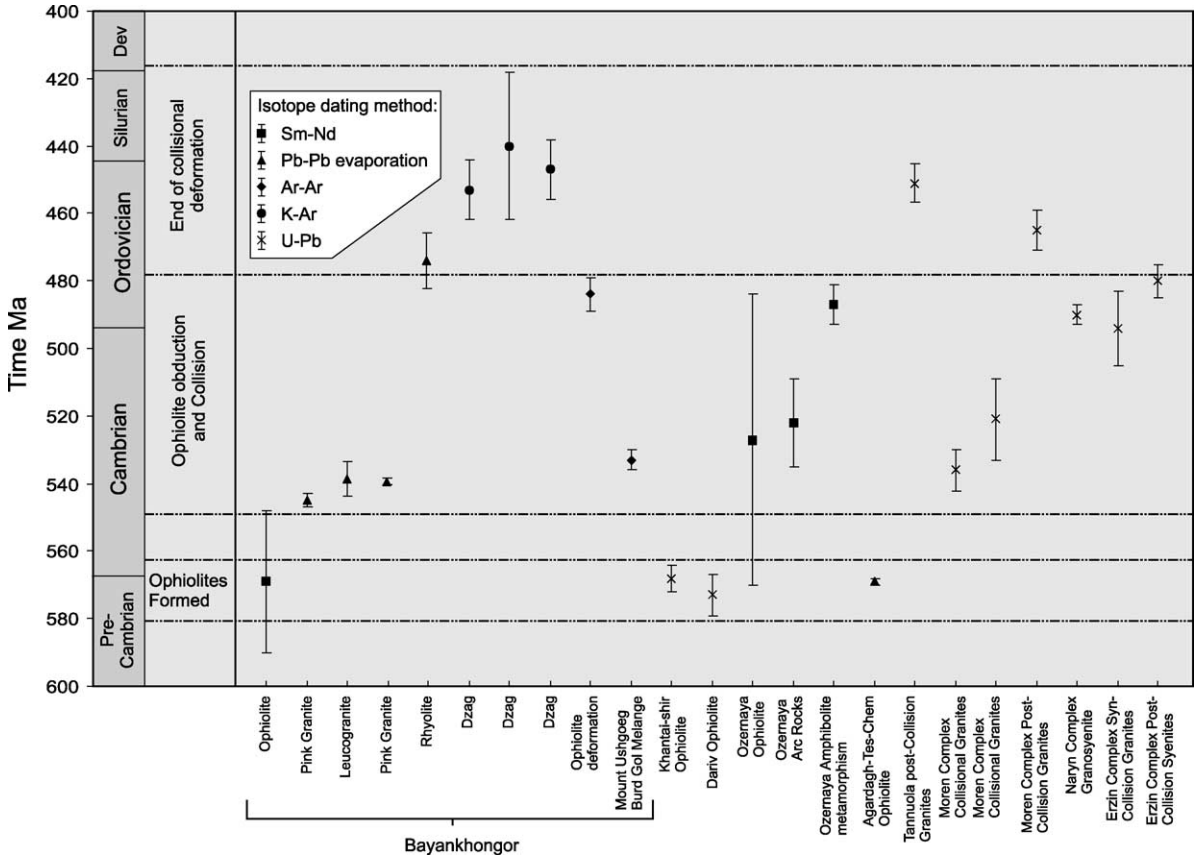

Fig. 10. Compilation of isotopic age data associated with Palaeozoic ophiolite belts in Western Mongolia and Southern Tuva. Isotopic ages for ophiolites group around 569 Ma and ages associated with collisional deformation suggest events at c. 540 and 450 Ma providing evidence of an arcuate belt from Bayankhongor to Agardagh Tes-Chem, which share a common deformation history. The difference in age and large error of the Ozernaya ophiolites could be associated with the effects of amphibolite metamorphism in this area. See Table 1 and Fig. 11 caption for data sources.

ocean. Höck et al. (2000) published an Ar–Ar plateau age of 533±3 Ma for biotite from a garnet–kyanite gneiss, which forms part of the Burd Gol mélange south of Mount Ushgoeg (Figs. 10 and 11, Table 2), which is comparable to the granite ages of this study. Because the Ar–Ar ages record the cooling phase of deformation, the data suggest that parts of the Burd Gol mélange experienced reasonably high-grade metamorphism associated with a regional deformation event at approximately the same time as the granites were produced, which is consistent with a collisional interpretation. Foliation of the leucogranite (97M123) along the thrust faults forming its northern margin (Fig. 2) suggests that it was either emplaced syn-tectonically and as a result was foliated, or deformed later by post-intrusion movement possibly during post-Carboniferous reactivation (Buchan et al., 2001). Also, K–Ar ages of cleavage forming white mica in the Dzag Zone (Kurimoto et al., 1998; Fig. 2, Table 1) near to its thrust contact with the ophiolite zone (Fig. 11) indicate that these micas cooled below their closure temperature around 450 Ma (Table 2). This suggests that deformation and associated metamorphism continued within the thrust zone between the Dzag and ophiolite zones. In addition, recent Ar–Ar data indicate that amphiboles developed on cleavage planes, associated with thrust deformation in pillow basalts of the Bayankhongor ophiolite formed around 485±6 Ma, suggesting that parts of the ophiolite were still undergoing deformation at this time (Delor et al.,

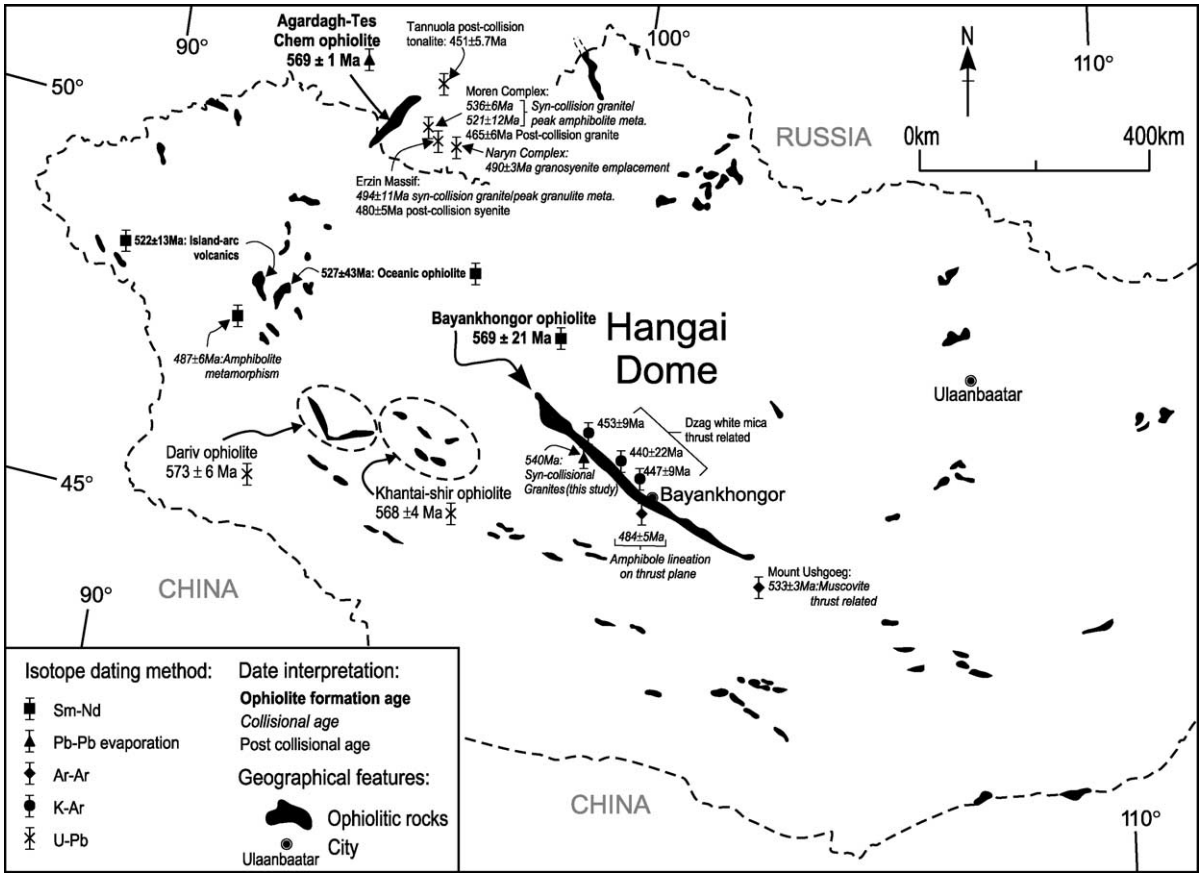

Fig. 11. Map of isotopic age data for ophiolites, collision-related granites and metamorphic rocks. The data demonstrate a strong correlation for the history of ophiolites in western Mongolian and southern Tuva. See Table 1 for Bayankhongor data sources. Other data sources: Tannuola (U–Pb zircon) (Kozakov et al., 1999), Moren, Erzin and Naryn complexes (U–Pb zircon) (Kozakov et al., 1999; Salnikova et al., 2001), Ozernaya (Sm–Nd whole rock and amphibole mineral isochron) (Kovalenko et al., 1996a) and Agardagh Tes-Chem (Pfänder et al., 1999).

2000; Figs. 10 and 11). Therefore, the c. 540 Ma event that produced the granites can be interpreted as an initial 'soft' collision, after which convergence continued with subduction of the Dzag passive margin and Hangai continent beneath the Burd Gol and Baidrag block. In this case, the rhyolite dykes may have intruded during the final stages of the collisional process before regional cooling began.

In summary, the combined isotope–geochronological data for the Bayankhongor area suggests that the Bayankhongor ophiolite was formed at 569 Ma. After a period of subduction–accretion lasting between 25 and 30 Ma, the ophiolite was accreted to the Burd Gol accretionary complex and subsequently obducted onto the Dzag passive margin during collision with the Hangai continent between 540 and 450 Ma (Fig. 10).

5.3. Regional constraints on deformation in the Central Asian Orogenic Belt

Geochronological data from ophiolites in western Mongolia and Tuva (southern Siberia) suggest that ophiolite rocks that cover a large area of what is now the CAOB may have been formed in one or more ocean basins at c. 570 Ma. Figs. 10 and 11 show the remarkable correlation for the ages of the Bayankhongor (569±21 Ma; Kepezhinskas et al., 1991), Khantaishir (568±4 Ma; E.B. Salnikova, personal communication), Dariv (573±6 Ma; Salnikova, personal communication), Ozernaya (527±43 Ma; Kovalenko et al., 1996a) and Agardagh Tes-Chem (569±1 Ma; Pfänder et al., 1999). These preserved remnants of oceanic crust occur along a gently curving semi-continuous belt of oceanic crust following the trace of basement structural grain, all of which, with the possible exception of the Ozernaya ophiolites, was produced around 570 Ma (Fig. 1). Kozakov et al. (1999) and Salnikova et al. (2001) carried out a detailed geochronological study of the geologically complex region to the east of the Agardagh Tes-Chem ophiolite (Fig. 10), which has previously been assumed to form part of a Precambrian microcontinent known as the Tuva–Mongolian Massif. They found that the Erzin Massif, Moren and Naryn complexes that make up this area were not metamorphosed in the Precambrian, as previously suggested by Mossakovsky et al. (1994), among others, but instead the earliest metamorphism in the Moren Massif took place around 536±6 Ma. From their analyses, they produced a detailed geochronological model for accretion and collision involving initial amalgamation of the three complexes between approximately 536 and 490 Ma followed by a prolonged period of deformation that ended with the intrusion of several postcollision granites and syenites at around 480–450 Ma (Figs. 10 and 11). The time scale proposed by these authors is similar to that suggested here for the Bayankhongor area, with initial 'soft' collision and ophiolite obduction at approximately 540 Ma and cessation of major regional deformation at around 450 Ma (Fig. 10). In addition, Kovalenko et al. (1996a) proposed that the Ozernaya island arcs and ophiolites (Fig. 11) were obducted and accreted at around 490 Ma based on a Sm–Nd age of 487±6 Ma for amphibolite metamorphism in the area (Figs. 10 and 11). These combined data sets for the western Mongolian and southwest Tuva ophiolites provide strong evidence for a regional correlation of a collisional suture and associated regional metamorphism and contractional/transpressional deformation. In addition, they define the margins of the Hangai cratonic nucleus (Fig. 1, inset) suggested by Cunningham (2001) to be a major control on the localisation of Cenozoic uplift and active growth of the Mongolian Altai mountain range, which lies to the west and southwest of the Hangai block. At present, detailed models for the genesis of the ophiolites is only available for the Bayankhongor ophiolite (Buchan et al., 2001, 2002) and Agardagh Tes–Chem ophiolite (Pfänder et al., 2002), making it difficult to produce a comprehensive reconstruction of the genetic relationships of these ophiolites in a singular ocean basin, or multiple coevally closing ocean basins. However, the data presented here indicate that a large part of the CAOB was formed at similar times and may also have been part of the same oceanic system prior to 540 Ma.

Acknowledgements

We thank the Institute for Geology and Mineral Resources (Mongolia) for their help in organising fieldwork and providing mapping materials. Constructive reviews by B. A. Natal'in and M. Sun led to improvement of the manuscript. C. Buchan is supported by a NERC PhD studentship no. GT04/

97/145/ES. B.F. Windley acknowledges NERC grant no. GR9/01881. Collaboration between the University of Leicester and Max-Planck-Intitut für Chemie was assisted by grants from the British Council-DAAD Academic Research Collaboration Programme (ARC grant 0964) and INTAS project 95 RUSSIA 0934. This manuscript forms ARC Tectonics Special Research Centre publication 186. **[RR]**

References

Andreas, D., 1970. Geological sheet map (L-47-55E, 56, 67E, 68). Open file report in Geological Funds of Mongolia no. 1895.

Arakawa, Y., Naito, K., Takahashi, Y., Oyungerel, S., Amakawa, H., 1998. Rb–Sr whole rock isochron age of Daltyn-am Complex in Bayankhongor area, central Mongolia. Mong. Geosci. 8, 16–19.

Arndt, N.T., Goldstein, S.L., 1987. Use and abuse of crust-formation ages. Geology 15 (10), 893–895.

Barth, M.G., McDonough, W.F., Rudnick, R.L., 2000. Tracking the budget of Nb and Ta in the continental crust. Chem. Geol. 165, 197–213.

Blevin, P.L., Chappell, B.W., 1995. Chemistry, origin, and evolution of mineralised granites in the Lachlan Fold Belt, Australia: the metallogeny of I- and S-type granites. Econ. Geol. 90, 1604–1619.

Buchan, C., 2002. Tectonic evolution of the Bayankhongor ophiolite, Central Mongolia: implications for the Palaeozoic crustal growth of Central Asia. PhD Thesis, University of Leicester, Leicester, 179 pp.

Buchan, C., Cunningham, D., Windley, B.F., Tomurhuu, D., 2001. Structural and lithological characteristics of the Bayankhongor ophiolite zone, Central Mongolia. J. Geol. Soc. (Lond.) 158, 445–460.

Buchan, C., Pfänder, J., Cunningham, D., Windley, B., 2002. Tectonic evolution of the Bayankhongor ophiolite, Central Mongolia: implications for the Palaeozoic crustal growth of Central Asia. In: Dilek, Y., Robinson, P.T. (Eds.), Ophiolites in Earth History. The Geological Society of London, London.

Chappell, B.W., White, A.J.R., 1992. I- and S-type granites in the Lachlan Fold Belt. Trans. R. Soc. Edinb. Earth Sci. 83, 1–26.

Cocherie, A., Guerrot, C., Rossi, P.H., 1992. Single-zircon dating by step-wise Pb evaporation: comparison with other geochronological techniques applied to the Hercynian granites of Corsica, France. Chem. Geol. 101, 131–141.

Coleman, R.G., 1989. Continental growth of Northwest China. Tectonics 8 (3), 621–635.

Cunningham, W.D., 2001. Cenozoic normal faulting and regional doming in the southern Hangay region, Central Mongolia: implications for the origin of the Baikal rift province. Tectonophysics 331 (4), 389–411.

Delor, C., Deroin, J.-P., Maluski, H., Tomurtogoo, O., 2000. Petrostructural constraints and Ar–Ar dating of the Bayankhongor ophiolites. In: Badarch, G., Jahn, B.-M. (Eds.), IGCP 420 Continental Growth in the Phanerozoic: Evidence from Central Asia, Second Workshop, Abstracts and Excursion Guidebook (Geotraverse Through a Terrane Collage in Southern Hangay) July 25–August 3, 1999, Ulaanbaatar, Mongolia. Geosciences Rennes, Hors serie n. 2, Rennes.

DePaolo, D.J., Linn, A.M., Schubert, G., 1991. The Continental crustal age distribution: methods of determining mantle separation ages from Sm–Nd isotopic data and application to the Southwestern United States. J. Geophys. Res. 96 (B2), 2071–2088.

Dergunov, A.B., Ryantsev, A.V., Luneva, O.I., Rikhter, A.V., 1997. Structure and Geological History of the Bayan–Khongor Zone, Central Mongolia. Geotectonics 31 (2), 132–140.

Goldstein, S.L., O'Nions, R.K., Hamilton, P.J., 1984. A Sm–Nd isotopic study of atmospheric dusts and particulates from major river systems. Earth Planet. Sci. Lett. 70, 221–236.

Harvey, P.K., Lovell, M.A., Brewer, T.S., Locke, J., Mansley, E., 1996. Measurement of thermal neutron absorption cross section in selected geochemical reference materials. Geostand. Newsl. 20, 79–85.

Höck, V., Frank, W., Hejl, E., Furtmueller, G., 2000. Petrology and cooling history of the Mt. Ushgoeg Range (Central Mongolia). In: Badarch, G., Jahn, B.-M. (Eds.), IGCP 420 Continental Growth in the Phanerozoic: Evidence from Central Asia, Second Workshop, Abstracts and Excursion Guidebook (Geotraverse Through a Terrane Collage in Southern Hangay) July 25–August 3 1999, Ulaanbaatar, Mongolia. Geosciences Rennes, Hors serie n. 2, Rennes.

Hofmann, A.W., 1988. Chemical differentiation of the Earth: the relationship between mantle, continental crust, and oceanic crust. Earth Planet. Sci. Lett. 90, 297–314.

Hsü, K.J., Qingcheg, W., Liang, L., Jie, H., 1991. Geological evolution of the neimonides: a working hypothesis. Eclogae Geol. Helv. 84 (1), 1–31.

Jacobsen, S.B., Wasserburg, G.J., 1980. Sm–Nd isotopic evolution of chondrites. Earth Planet. Sci. Lett. 50, 139–155.

Jahn, B.-M., Griffin, W.L., Windley, B.F., 2000. Continental Growth in the Phanerozoic: evidence from Central Asia. Tectonophysics 328 (1–2), 1–6.

Kepezhinskas, P.K., Kepizhinskas, K.B., Pukhtel, I.S., 1991. Lower Plaeozoic oceanic crust in Mongolian Caledonides: Sm–Nd isotope and trace element data. Geophys. Res. Lett. 18, 1301–1304.

Kober, B., 1987. Single-zircon evaporation combined with Pb^+ emitter bedding for $^{207}Pb/^{206}Pb$-age investigations using thermal ion mass spectrometry, implications to zirconology. Contrib. Mineral. Petrol. 96, 63–71.

Kovalenko, V.I., et al., 1996. The Sm–Nd Isotopic systematics of ophiolites in the Ozernaya Zone (Mongolia). Stratigr. Geol. Correl. 4 (2), 107–113.

Kovalenko, V.I., et al., 1996. Sources of Phanerozoic granitoids in Central Asia: Sm–Nd isotope data. Geochem. Int. 34 (8), 628–640.

Kozakov, I.K., Kotov, A.B., Kovach, V.P., Salnikova, E.B., 1997. Crustal growth in the geologic evolution of the Baidarik Block, Central Mongolia: evidence from Sm–Nd isotopic systematics. Petrology 5 (3), 201–207.

Kozakov, I.K., Salnikova, E.B., Kotov, A.B., Kröner, A., Zagornaya, N.Y., 1999. Latest Neoproterozoic to early Palaeozoic crustal accretion in southern Siberia: a reinterpretation of the Tuvino–Mongolian Massif. J. Conf. Abstr., Terra Abstr., Eur. Union Geosci. 4 (1), 109.

Kröner, A., Todt, W., 1988. Single zircon dating constraining the maximum age of the Barberton greenstone belt, Southern Africa. J. Geophys. Res. 93 (B12), 15329–15337.

Kröner, A., Byerly, C.R., Lowe, D.R., 1991. Chronology of early Archaean granite–greenstone evolution in the Barberton Mountain Land, South Africa, based on precise dating by single zircon evaporation. Earth Planet. Sci. Lett. 103, 41–54.

Kröner, A., Windley, B.F., Jaeckel, P., Brewer, T.S., Razakamanana, T., 1999. New Zircon ages and regional significance for the evolution of the Pan-African orogen in Madagascar. J. Geol. Soc. (Lond.) 156, 1125–1135.

Kurimoto, C., Tungalag, F., Bayarmandal, L., Ichinnorov, N., 1998. K–Ar ages of white micas from pelitic schists of the Bayankhongor area, west Mongolia. Bull. Geol. Surv. Jpn. 49 (1), 19–23.

Lamb, M.A., Badarch, G., 1997. Palaeozoic sedimentary basins and volcanic-arc systems of southern Mongolia: new stratigraphic and sedimentologic constraints. Int. Geol. Rev. 39, 542–576.

Mitrofanov, F.P., Kozakov, I.K., Palay, I.P., 1981. Precambrian of west Mongolia and South Tuva. Transactions of The Joint Soviet–Mongolian Scientific-Research Geological Expedition, vol. 32. Nauka, Leningrad, pp. 90–102.

Mitrofanov, F.P., et al., 1985. Isotope age of "grey" tonalites and gneisses of the Archean in Caledonian Structures of central Mongolia. Dokl. Akad. Nauk SSSR 284 (3), 670–675.

Moores, E.M., 1970. Ultramafics and orogeny, with models for the U.S. Cordillera and Tethys. Nature 228, 837–842.

Mossakovsky, A.A., Ruzhentsev, S.V., Samygin, S.G., Kheraskova, T.N., 1994. Central Asian Fold Belt: geodynamic evolution and formational history. Geotectonics 27 (6), 445–474.

O'Nions, R.K., Hamilton, P.J., Hooker, P.J., 1983. A Nd isotope investigation of sediments related to crustal development in the British Isles. Earth Planet. Sci. Lett. 63, 229–240.

Oyungerel, S., 1998. Petrography of the granitoids in Bayankhongor area. Mong. Geosci. 8, 4–15.

Oyungerel, S., Takahashi, Y., 1999. New radiometric data of the granitoids in Bayankhongor area, central Mongolia. Mong. Geosci. 13, 38–40.

Pfänder, J., Jochum, K.P., Todt, W., Kröner, A., 1999. Relationships between the mantle, lower crust and upper crust within the Agardagh-Tes Chem Ophiolite, Central Asia: evidence from petrologic, trace element, and isotopic data. Ofioliti 24 (1a), 151–152.

Pfänder, J.A., Jochum, K.P., Kozakov, I.K., Kröner, A., Todt, W., 2002. Coupled evolution of black-arc and island arc like mafic crust in the late-Neoproterozoic Agardagh Tes-Chem ophiolite, Central Asia: evidence from trace element and Sr–Nd–Pb isotope data. Contrib. Mineral. Petrol. 143 (2), 154–174.

Pidgeon, R.T., et al., 1994. Calibration of the CZ3 zircon standard for the Curtin SHRIMP II. US Geol. Surv. Circ. 1107, 251.

Plank, T., Langmuir, C.H., 1998. The chemical composition of subducting sediment and its consequences for the crust and mantle. Chem. Geol. 145, 325–394.

Salnikova, E.B., et al., 2001. Age of Palaeozoic granites and metamorphism in the Tuvino–Mongolian Massif of the Central Asian Mobile Belt: loss of a Precambrian microcontinent. Precambrian Res. 110, 143–164.

Şengör, A.M.C., Natal'in, B.A., Burtman, V.S., 1993. Evolution of the Altaid tectonic collage and Palaeozoic crustal growth in Eurasia. Nature 364, 299–307.

Sun, S.S., McDonough, W.F., 1989. Chemical and isotopic systematics of oceanic basalts: implications for mantle composition and processes. In: Saunders, A.D., Norry, M.J. (Eds.), Magmatism in Ocean Basins. Geological Society of London Special Publication, vol. 42. The Geological Society, London, pp. 313–345.

Takahashi, Y., Oyungerel, S., Naito, K., Delgertsogt, B., 1998a. Geology and magnetic susceptibility of the granitoids in Bayankhongor area, central Mongolia. Mong. Geosci. 7, 10–19.

Takahashi, Y., Oyungerel, S., Naito, K., Delgertsogt, B., 1998b. The granitoid series in Bayankhongor area, central Mongolia. Bull. Geol. Surv. Jpn. 49 (1), 25–32.

Takahashi, Y., Oyungerel, S., Naito, K., Delgertsogt, B., 1998c. Mineralogical characteristics of feldspars of the granitoids in Bayankhongor area, central Mongolia. Bull. Geol. Surv. Jpn. 49 (8), 439–446.

Tarney, J., Marsh, N.G., 1991. Major and trace element geochemistry of holes CY-1 and CY-4: implications for petrogenetic models. In: Gibson, I.L., Malpas, J., Robinson, P.T., Xenophontos, C. (Eds.), Initial Reports of the Cyprus Crustal Study. Geological Survey of Canada, Ottawa, pp. 133–176.

Teraoka, Y., Suzuki, M., Tungalag, F., Ichinnorov, N., Sakamaki, Y., 1996. Tectonic framework of the Bayankhongor area, West Mongolia. Bull. Geol. Surv. Jpn. 47 (9), 447–455.

Thompson, A.B., 1999. Some time–space relationships for crustal melting and granitic intrusion at various depths. In: Castro, A., Fernández, C., Vigneresse, J.L. (Eds.), Understanding Granites: Integrating New and Classical Techniques. Geological Society Special Publication No. 168. Geological Society, London, London, pp. 7–26.

Tungalag, F., 1996. Stratigraphy and structural geology of Precambrian and Palaeozoic Strata in Bayankhongor Area. Mong. Geosci. 1 (3), 4–11.

Watson, E.B., Harrison, T.M., 1983. Zircon saturation revisited—temperature and composition effects in a variety of crustal magma types. Earth Planet. Sci. Lett. 64, 295–304.

Whalen, J.B., Currie, K.L., Chappell, B.W., 1987. A-type granites: geochemical characteristics, discrimination and petrogenesis. Contrib. Mineral. Petrol. 95, 407–419.

Windley, B.F., Allen, M.B., 1993. Mongolian plateau—evidence for a late Cenozoic mantle plume under central-Asia. Geology 21 (4), 295–298.

Zabotkin, L.B., 1988. Geological sheet map (L-47-XXIII and XXIV). Open file report in Geological Funds of Mongolia no. 4276.

Zen, E.-A., 1986. Aluminium enrichment in silicate melts by fractional crystallization: some mineralogical and petrographic constraints. J. Petrol. 27, 1095–1117.